Frontiers of Information Technology & Electronic Engineering
www.jzus.zju.edu.cn; engineering.cae.cn; www.springerlink.com
ISSN 2095-9184 (print); ISSN 2095-9230 (online)
E-mail: jzus@zju.edu.cn

An improved sliding mode control based on fuzzy logic for quadrotor unmanned aerial vehicles under unmatched uncertainty*#

Qingmei CAO†‡1, Ruiwen XIANG1, Yonghong TAN†2, Weiqing SUN†1, Jiawei CHI1, Xiaodong ZHOU†3,4, Lei YAO1

[1]School of Mechanical Engineering, University of Shanghai for Science and Technology, Shanghai 200093, China
[2]College of Mechanical and Electronic Engineering, Shanghai Normal University, Shanghai 200234, China
[3]School of Information and Cyber Security, People's Public Security University of China, Beijing 100038, China
[4]Department of Informatization and Cyber Security, Shanghai Police College, Shanghai 200137, China
†E-mail: cqm@usst.edu.cn; tany@shnu.edu.cn; sunwq@usst.edu.cn; zhouxdshpc@163.com

Received Jan. 25, 2025; Revision accepted July 7, 2025; Crosschecked Aug. 20, 2025; Published online Nov. 6, 2025

Abstract: A novel fuzzy sliding mode control (FSMC) strategy is proposed to enhance the robustness and stability of position control for underactuated quadrotor unmanned aerial vehicles (UAVs) in the presence of external disturbances and model uncertainties. To realize the adaptive ability and robustness of the system in complex dynamic environments, an intelligent two-dimensional fuzzy controller is designed based on traditional sliding mode control (SMC) to adjust SMC parameters in real time, thereby adapting to the variable structure parameters of the system. First, based on the designed filter variables regarding errors, traditional SMC is used to reduce tracking errors. Then, the fuzzy logic module (FLM) combined with SMC, i.e., the self-learning module (FLM+SMC), is developed based on the filter variables and their rate of change to adjust the two parameters of the above SMC. Subsequently, the output signals of the FLM are fed back into the SMC module, and then a closed-loop tuning system using FSMC is developed for the UAVs. Moreover, the stability of the FSMC is rigorously verified using the Lyapunov theory. Finally, comprehensive simulations demonstrate that the designed FSMC not only offers accurate trajectory precision but also has robustness and disturbance rejection, and comparative simulations using SMC and adaptive radial basis function neural network control (RBFNNC) are used to validate the result.

Key words: Sliding mode control; Fuzzy logic theory; Underactuated system; Unmanned aerial vehicle; Self-learning strategy
https://doi.org/10.1631/FITEE.2500058 **CLC number:** TP301

1 Introduction

In the era of rapid development of unmanned aerial vehicle (UAV) technology, UAV technology has demonstrated widespread potential across various sectors, including military, civil, scientific research, and energy (Du et al., 2019; Li et al., 2024). For instance, within the energy sector, there has been a growing emphasis on enhancing efficiency and reducing costs in recent years to better adapt

‡ Corresponding author
* Project supported by the National Natural Science Foundation of China (Nos. 61971120, 62171285, 62033009, and 62327807) and the National Key Research and Development Program of China (No. 2021YFC2801300)
# Electronic supplementary materials: The online version of this article (https://doi.org/10.1631/FITEE.2500058) contains supplementary materials, which are available to authorized users
ORCID: Qingmei CAO, https://orcid.org/0000-0002-1661-9225

to the evolving environmental conditions. Vehicle technology, particularly its trajectory tracking capabilities, offers novel opportunities for the energy sector, enabling safer and more efficient operations, maintenance, and monitoring in areas like wind and solar energy (Amer et al., 2023; Rahbari et al., 2024). However, the intrinsic characteristics of UAVs, such as strong coupling, nonlinearity, and underactuation (Guo et al., 2022; Wang F et al., 2024), combined with model uncertainties arising from dynamic external environments, result in complex nonlinear dynamics, presenting significant challenges for modeling and control design. This study focuses on quadrotor UAVs as the research object, and examines the position tracking problem of UAVs.

As a widely-used classic linear control algorithm, the proportional–integral–derivative (PID) controller adjusts three weight coefficients, e.g., proportional, integral, and derivative, to control the output variable and bring it closer to the setpoint (Pounds et al., 2012; Nair et al., 2016). For example, Ermeydan and Kiyak (2017) proposed an enhanced PID controller to study fault-tolerant control of quadrotors, which solves the flight stability problem caused by one or more actuator failures. With the development of intelligent technology, PID control is combined with other intelligent methods. For example, Santoso et al. (2021) proposed a hybrid nonlinear control system with a traditional proportional–differential (PD) controller and PD fuzzy logic. This system combines the numerical simulation with real-time flight tests to solve the problem of insufficient control accuracy in the trajectory tracking of quadrotor UAVs. Mendoza and Yu (2023) proposed a new fuzzy adaptive neural PID controller, which was tested using a fuzzy adaptive control law simulation to solve the control accuracy and stability issues in trajectory tracking of small-scale UAVs. However, in nonlinear systems, especially quadrotors with both nonlinear and strong coupling characteristics, PID controllers may not provide sufficient control accuracy within a local operating range near nonlinear points.

As a classic nonlinear control strategy, compared to PID control, sliding mode control (SMC) is more suitable for handling nonlinear, time-varying, and easily disturbed systems compared to PID control. It can improve the transient and steady-state performance of the system. SMC achieves precise trajectory tracking of UAVs by quickly converging on a sliding mode surface, and therefore it is widely used in various systems (Wang T et al., 2014). Meanwhile, to further enhance the robustness and other performance of SMC, exploring its combination with other algorithms has become an important direction in SMC research. For example, Chen FY et al. (2016) proposed a robust nonlinear controller with a dual-loop structure, which combines SMC with backstepping control to solve the control problem of quadrotor UAVs in Cartesian position trajectory tracking. The simulation results showed that the method has good robustness and tracking performance. Nguyen et al. (2021) proposed an SMC method for quadrotor systems under external disturbances. This method incorporates a neural network-adjusted time-varying sliding mode surface for dynamic gain adaptation via backpropagation, coupled with a disturbance observer to estimate and compensate for external disturbances. Finally, the stability of the control method is verified using the Lyapunov theory, demonstrating superior tracking performance and anti-interference ability compared to traditional SMC. Yu et al. (2022) proposed a new non-singular fixed-time sliding mode surface and a continuous fast fixed-time SMC law; the robustness and stability problems of UAVs under parameter uncertainty and external disturbances were solved. However, during the operation of SMC, due to the discontinuity of its control law, oscillations are easily generated, which can have adverse effects on the actual performance and stability of the controller (Chen FY et al., 2016).

Neural network control (NNC) is a powerful machine learning method that can effectively learn and model complex nonlinear relationships. This algorithm has excellent adaptability and generalization ability, thus exhibiting flexible control capability in dynamic systems. Compared with SMC, NNC can automatically adjust the control strategy when dealing with system changes, without the need to redesign the controller or manually adjust parameters. This characteristic of NNCs is particularly prominent in dealing with nonlinear control problems, especially in application scenarios that face challenges such as data scarcity or frequent environmental changes (Nodland et al., 2013; Rao et al., 2022; Yang L et al., 2023). In view of the characteristics of self-learning and nonlinear approximation, radial basis function neural network control (RBFNNC) is widely used to compensate for uncertain items to improve the robustness and adaptability (Chen PY et al., 2021; Shen and Xu, 2021). Chen PY et al. (2021) introduced an RBFNNC model into S-plane control. The S-plane module achieves a parameter adaptive adjustment function, solving the problem of parameter coefficient setting in fixed-wing UAV attitude control, relying entirely on experience and being unable to adjust adaptively. Shen and Xu (2021) proposed an active disturbance rejection controller based on RBFNNC. They established a state observer using the modern control theory and estimated the unknown total disturbance using an adaptive radial basis function (RBF) neural network. Finally, the simulation results showed that this method has good anti-interference and robustness. However, RBFNNC requires a large amount of data for training to achieve excellent generalization ability, and the training is also time-consuming.

In summary, designing variable structure control systems for UAVs has emerged as a mainstream trend in scientific research. While significant advancements have been made in enhancing tracking accuracy, several critical challenges remain unaddressed. One major issue is the insufficient emphasis on system robustness in some studies (Yu et al., 2022; Mendoza and Yu, 2023). This oversight can lead to substantial degradation in system performance under practical conditions, potentially compromising overall system stability. Moreover, the complex and dynamic nature of wind conditions and air disturbances in real-world flight environments is often either overlooked (Chen FY et al., 2016; Ermeydan and Kiyak, 2017) or overly simplified into constant terms (Nguyen et al., 2021). Such simplifications limit the applicability and effectiveness of the proposed control algorithms in complex and dynamic environments.

To overcome the limitations of the aforementioned UAV control algorithms, this paper proposes a fuzzy sliding mode control (FSMC) strategy, specifically for the position tracking problem of quadrotor UAVs with complex dynamics. A nonlinear model that encapsulates disturbances and parameter uncertainties is constructed in the proposed FSMC method, and an exponential convergence-based sliding mode controller is integrated, enabling nonlinear tracking of the system. Based on this, fuzzy control is designed for the adaptive tuning of sliding mode parameters, which not only improves tracking accuracy but also enhances the corresponding dynamic performance.

The main contributions to this work are as follows:

1. Designing an intelligent framework using a fuzzy logic module (FLM, two-dimensional), i.e., FLM+SMC, for controlling parameters, realizing self-learning adjustment of parameters in the local range of nonlinear operating points under the condition of unmatched external interference.

2. The observation signal is obtained by using interference information statistics. The control strategy, using the interference feedback signal as control input information, is designed by combining the above feedback observation with Lyapunov stability analysis, thereby improving the robustness of the UAV.

2 System dynamics

A quadrotor UAV can be defined as a type of adversarial structure driven by four electric motors installed on the corresponding rotors (R_1–R_4). The simplified dynamic model of a quadrotor UAV is shown in Fig. 1, where the coordinate system $B=\{x_\mathrm{b}, y_\mathrm{b}, z_\mathrm{b}\}$ represents the body coordinate system, and $E=\{x_\mathrm{e}, y_\mathrm{e}, z_\mathrm{e}\}$ is the Earth coordinate system. The Euclidean position angle and Euler angle of the UAV relative to the coordinate system E are represented by $\boldsymbol{\chi} \triangleq [x, y, z]^\mathrm{T} \in \mathbb{R}^3$ and $\boldsymbol{p} \triangleq [\phi, \theta, \psi]^\mathrm{T} \in \mathbb{R}^3$, respectively.

Under the assumption that the UAV to be studied in this present paper is a rigid body, the dynamic mathematical description can be derived via

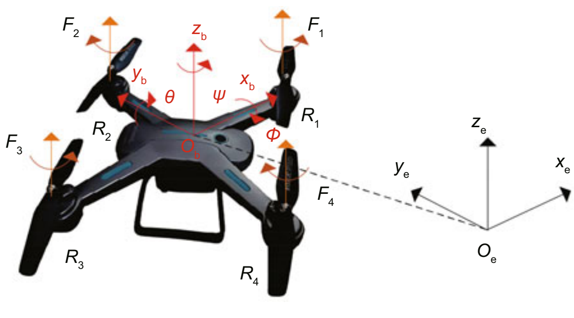

Fig. 1 Schematic of the quadrotor system

the Newton–Euler formula (Song et al., 2019):

$$\begin{cases}\ddot{x}=(\cos\phi\sin\theta\cos\psi+\sin\phi\sin\psi)F_{\rm at}/m-\xi_x\dot{x}/m,\\ \ddot{y}=(\cos\phi\sin\theta\sin\psi-\sin\phi\sin\psi)F_{\rm at}/m-\xi_y\dot{y}/m,\\ \ddot{z}=(\cos\phi\cos\theta)F_{\rm at}/m-g-\xi_z\dot{z}/m,\\ \ddot{\phi}=\dot{\theta}\dot{\psi}\frac{(I_y-I_z)}{I_x}-\frac{I_{\rm r}}{I_x}\dot{\theta}\bar{\omega}-\frac{\xi_\phi}{I_x}\dot{\phi}+\frac{1}{I_x}\tau_{{\rm a}\phi},\\ \ddot{\theta}=\dot{\phi}\dot{\psi}\frac{(I_z-I_x)}{I_y}-\frac{I_{\rm r}}{I_y}\dot{\phi}\bar{\omega}-\frac{\xi_\theta}{I_y}\dot{\theta}+\frac{1}{I_y}\tau_{{\rm a}\theta},\\ \ddot{\psi}=\dot{\phi}\dot{\theta}\frac{(I_x-I_y)}{I_z}-\frac{\xi_\psi}{I_z}\dot{\psi}+\frac{1}{I_z}\tau_{{\rm a}\psi},\end{cases} \tag{1}$$

where m is the mass of the UAV, and g is the gravitational acceleration. ξ_x, ξ_y, ξ_z and ξ_ϕ, ξ_θ, ξ_ψ are aerodynamic damping coefficients; I_x, I_y, and I_z are the moments of inertia; $I_{\rm r}$ is the rotor inertia; $F_{\rm at}$, $\tau_{{\rm a}\phi}$, $\tau_{{\rm a}\theta}$, and $\tau_{{\rm a}\psi}$ represent the control thrust and three control torques generated by four rotors; $\overline{\omega}=\omega_4+\omega_3-\omega_2-\omega_1$ denotes the overall residual rotor angular, which is treated as an unknown bounded disturbance frequently.

Remark 1 Based on the definition of control thrust

$$F_{\rm at}=\kappa(\omega_1^2+\omega_2^2+\omega_3^2+\omega_4^2), \tag{2}$$

along with the control torques

$$\tau_{{\rm a}\phi}=\kappa l(\omega_3^2-\omega_1^2), \tag{3a}$$

$$\tau_{{\rm a}\psi}=b(\omega_1^2+\omega_2^2+\omega_3^2+\omega_4^2), \tag{3b}$$

$$\tau_{{\rm a}\theta}=\kappa l(\omega_4^2-\omega_2^2), \tag{3c}$$

where κ is the reverse moment coefficient, l is the rotor arm length, and b is the drag torque coefficient. The quadrotor can be defined as a form of underactuated dynamics for the four input variables $[u_1,u_2,u_3,u_4]^{\rm T}=[F_{\rm at},\tau_{{\rm a}\phi},\tau_{{\rm a}\psi},\tau_{{\rm a}\theta}]^{\rm T}$ and six output variables $[x,y,z,\phi,\psi,\theta]^{\rm T}$ in the UAVs.

Considering that the noise from the sensors and the uncertainty from the external environment can seriously affect tracking accuracy, the corresponding external disturbances

$$\boldsymbol{d}_{\rm ext}(\cdot)=[d_x(\cdot),d_y(\cdot),d_z(\cdot)]^{\rm T}\in\mathbb{R}^3 \tag{4}$$

have been taken into account, and then the following dynamic description

$$\ddot{\boldsymbol{\chi}}=\boldsymbol{A}\boldsymbol{u}_{\rm s}(t)+\boldsymbol{f}_1(\cdot)+\boldsymbol{d}_{\rm ext}(\boldsymbol{\chi},t) \tag{5}$$

is established based on Eq. (2), where $\boldsymbol{u}_{\rm s}=[Q_x,Q_y,Q_z]^{\rm T}$, $\boldsymbol{A}$ and $\boldsymbol{f}_1(\cdot)$ are detailed in Eqs. (6a) and (6b), given by

$$\boldsymbol{A}=\begin{bmatrix}a_4&0&0\\0&a_4&0\\0&0&a_4\end{bmatrix}\in\mathbb{R}^{3\times3}, \tag{6a}$$

$$\boldsymbol{f}_1(\cdot)=\begin{pmatrix}-a_1\dot{x}\\-a_2\dot{y}\\-a_3\dot{z}-g\end{pmatrix}\in\mathbb{R}^{3\times1}, \tag{6b}$$

$a_1=\frac{\xi_x}{m}$, $a_2=\frac{\xi_y}{m}$, $a_3=\frac{\xi_z}{m}$, and $a_4=\frac{1}{m}$.

For the convenience of the subsequent controller design, Q_x, Q_y, and Q_z are designed in Eq. (7), which represent virtual control inputs for longitudinal, transverse, and altitude channels, respectively (Jiang, 2021):

$$\begin{cases}Q_x=(\cos\phi\sin\theta\cos\psi+\sin\psi\sin\phi)u_1,\\ Q_y=(\cos\phi\sin\theta\sin\psi-\sin\phi\cos\psi)u_1,\\ Q_z=(\cos\phi\cos\theta)u_1,\end{cases} \tag{7}$$

where $u_1=F_{\rm at}$ denotes the total thrust, which is introduced here to simplify the subsequent control design formulation.

Assumption 1 The parameters a_1–a_4 in Eq. (6) are unknown but bounded.

Assumption 2 The external disturbance $\boldsymbol{d}_{\rm ext}(\cdot)$ is bounded, satisfying $|d_x(\cdot)|\le\bar{d}_x$, $|d_y(\cdot)|\le\bar{d}_y$, and $|d_z(\cdot)|\le\bar{d}_z$, where $\bar{d}_x$, $\bar{d}_y$, and $\bar{d}_z$ are the elements of the unknown constant vector $\bar{\boldsymbol{d}}_{\rm ext}=[\bar{d}_x,\bar{d}_y,\bar{d}_z]^{\rm T}$.

3 Controller design and stability analysis

Given that the main task of this research is UAV tracking in complex variable environments, the core problem involves designing a variable-structure nonlinear controller. Above all, a suitable SMC module is designed as the core framework of the system. Subsequently, a fuzzy control module is further integrated based on the SMC design framework and fuzzy logic reasoning. Thus, the stability of the proposed FSMC is rigorously verified using the Lyapunov function. The control structure principle for the designed FSMC strategy for position tracking accuracy is shown in Fig. 2.

The so-called FSMC strategy integrates the fuzzy logic unit (13) into SMC submodel (14) under the external disturbances $\boldsymbol{d}_{\rm ext}(\boldsymbol{\chi},t)$. For achieving accurate tracking effect, the actual output $\boldsymbol{\chi}$, tracking error $\boldsymbol{e}_{\boldsymbol{\chi}}$, and their rates of change $(\dot{\boldsymbol{\chi}},\dot{\boldsymbol{e}}_{\boldsymbol{\chi}})$, along

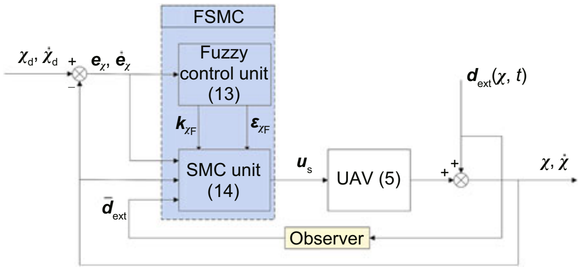

Fig. 2 Structural diagram of the UAV system

with the upper bound of external disturbances $\bar{\boldsymbol{d}}_{\mathrm{ext}}$, are designed as the inputs of the submodel of the fuzzy logic. Then, the logic unit is used to update the self-learning parameters, i.e., $\boldsymbol{\varepsilon}_{\boldsymbol{\chi}_\mathrm{F}}$ and $\boldsymbol{k}_{\boldsymbol{\chi}_\mathrm{F}}$. Finally, the proposed FSMC, a strategy that combines the characteristics of parameter adaptive control and variable-structure sliding mode nonlinear control, is developed. The corresponding stability of the FSMC system is rigorously verified through the application of theoretical analysis methods.

3.1 Intelligent controller design for FSMC

Based on the defined tracking error

$$\boldsymbol{e}_{\boldsymbol{\chi}} = \boldsymbol{\chi} - \boldsymbol{\chi}_\mathrm{d} \tag{8}$$

and the sliding mode surface

$$\boldsymbol{s}_{\boldsymbol{\chi}} = \boldsymbol{c}_{\boldsymbol{\chi}} \boldsymbol{e}_{\boldsymbol{\chi}} + \dot{\boldsymbol{e}}_{\boldsymbol{\chi}}, \tag{9}$$

the nonlinear controller is designed with the environment adaptive capability. Herein, $\boldsymbol{\chi}_\mathrm{d}$ is the expected tracking trajectory of the UAVs, and $\boldsymbol{c}_{\boldsymbol{\chi}} > 0$ is a user-defined parameter for the SMC module within the FSMC system. Thus, the exponential approach law

$$\dot{\boldsymbol{s}}_{\boldsymbol{\chi}} = -\boldsymbol{\varepsilon}_{\boldsymbol{\chi}_\mathrm{F}} \mathbf{sat}(\boldsymbol{s}_{\boldsymbol{\chi}}) - \boldsymbol{k}_{\boldsymbol{\chi}_\mathrm{F}} \boldsymbol{s}_{\boldsymbol{\chi}} + \bar{\boldsymbol{d}}_{\mathrm{ext}} \tag{10}$$

can be developed. The other two input parameters of the SMC module are $\boldsymbol{\varepsilon}_{\boldsymbol{\chi}_\mathrm{F}} = \boldsymbol{\varepsilon}_{\boldsymbol{\chi}_{\mathrm{Fuzzy}(\boldsymbol{e},\dot{\boldsymbol{e}})}} > 0$ and $\boldsymbol{k}_{\boldsymbol{\chi}_\mathrm{F}} = \boldsymbol{k}_{\boldsymbol{\chi}_{\mathrm{Fuzzy}(\boldsymbol{e},\dot{\boldsymbol{e}})}} > 0$, which are directly generated by the fuzzy control module through fuzzy rule inference based on the position error $\boldsymbol{e}_{\boldsymbol{\chi}}$ and its rate of change $\dot{\boldsymbol{e}}_{\boldsymbol{\chi}}$ of the UAV. The specific formula for the saturation function $\mathbf{sat}(\boldsymbol{s}_{\boldsymbol{\chi}})$ can be chosen as

$$\mathbf{sat}(\boldsymbol{s}_{\boldsymbol{\chi}}) = \begin{cases} \mathbf{1}, & \boldsymbol{s}_{\boldsymbol{\chi}} > \boldsymbol{\Delta}_{\boldsymbol{\chi}}, \\ \boldsymbol{s}_{\boldsymbol{\chi}}/\boldsymbol{\Delta}_{\boldsymbol{\chi}}, & |\boldsymbol{s}_{\boldsymbol{\chi}}| \le \boldsymbol{\Delta}_{\boldsymbol{\chi}}, \\ -\mathbf{1}, & \boldsymbol{s}_{\boldsymbol{\chi}} < -\boldsymbol{\Delta}_{\boldsymbol{\chi}}, \end{cases} \tag{11}$$

where the bounded saturation function parameters satisfy $0 < \boldsymbol{\Delta}_{\boldsymbol{\chi}} \le \sup \boldsymbol{\Delta}$, and "sup" denotes the supremum operator.

Remark 2 A novel FLM is developed based on the tracking error $\boldsymbol{e}_{\boldsymbol{\chi}}$ and its rate of change $\dot{\boldsymbol{e}}_{\boldsymbol{\chi}}$ for tuning $\boldsymbol{\varepsilon}_{\boldsymbol{\chi}_\mathrm{F}}$ and $\boldsymbol{k}_{\boldsymbol{\chi}_\mathrm{F}}$, which can achieve self-learning for UAVs in complex and uncertain circumstances.

To overcome the trade-off between anti-interference and high-frequency flutter in the traditional SMC control strategy, fuzzy logic with self-learning ability is adopted to upgrade the traditional SMC, meanwhile, enhancing the uncertainty processing ability, self-adaptability, and system robustness. Thus, in the proposed FSMC strategy, the system position error $\boldsymbol{e}_{\boldsymbol{\chi}}$ and its rate of change $\dot{\boldsymbol{e}}_{\boldsymbol{\chi}}$ are selected as input parameters for fuzzy control, while the key tuning parameters $\boldsymbol{\varepsilon}_{\boldsymbol{\chi}_\mathrm{F}}$ and $\boldsymbol{k}_{\boldsymbol{\chi}_\mathrm{F}}$ in FSMC are used as output targets for fuzzy control. Subsequently, using the abundant database and knowledge-base resources, combined with expert experience and a deep understanding of the dynamic characteristics of the system, fuzzy logic rules are formulated within the SMC framework. Based on Fig. 2, the designed rule establishes a fuzzy relationship between the inputs $\boldsymbol{e}_{\boldsymbol{\chi}}$, $\dot{\boldsymbol{e}}_{\boldsymbol{\chi}}$ and the outputs $\boldsymbol{\varepsilon}_{\boldsymbol{\chi}_\mathrm{F}}$, $\boldsymbol{k}_{\boldsymbol{\chi}_\mathrm{F}}$. This process realizes the intelligent tuning of SMC parameters, enabling the control system to adjust the control strategy more flexibly and accurately in the face of modeling uncertainty and external disturbances.

Remark 3 Based on the basic physical characteristics of these two input parameters $\boldsymbol{e}_{\boldsymbol{\chi}}$ and $\dot{\boldsymbol{e}}_{\boldsymbol{\chi}}$, the corresponding fuzzy domains in fuzzy logic are determined, and appropriate fuzzification with a fuzzy quantization factor

$$\boldsymbol{k}_{\boldsymbol{i}} = \frac{\boldsymbol{i}_{\max} - \boldsymbol{i}_{\min}}{\boldsymbol{i}^*_{\max} - \boldsymbol{i}^*_{\min}} \tag{12}$$

is selected to reflect the mapping relationship between the fundamental domain $[\boldsymbol{i}^*_{\min}, \boldsymbol{i}^*_{\max}]$ and the fuzzy domain $[\boldsymbol{i}_{\min}, \boldsymbol{i}_{\max}]$, where $\boldsymbol{i} \in \{\boldsymbol{e}_{\boldsymbol{\chi}}, \dot{\boldsymbol{e}}_{\boldsymbol{\chi}}\}$.

During the process of fuzzy parameters in the proposed FSMC, the error of position tracking $\boldsymbol{e}_{\boldsymbol{\chi}}$ along with the rate of its change $\dot{\boldsymbol{e}}_{\boldsymbol{\chi}}$ are set as the input of the designed FSMC, and the parameters $\boldsymbol{\varepsilon}_{\boldsymbol{\chi}_\mathrm{F}}$ and $\boldsymbol{k}_{\boldsymbol{\chi}_\mathrm{F}}$, which need to be adjusted using the self-learning module, i.e., FLM+SMC, are used as the output of the FSMC. To solve the fuzzy processing in the FLM mechanism, the Mamdani fuzzy reasoning method and the centroid method are adopted in the FSMC. Moreover, for ensuring that the fuzzy controller can accurately and effectively capture the dynamic characteristics of the system, the fuzzy subset of the input variables is described as {NB, NS, Z, PS, PB}, representing negative big, negative small, zero, positive small, and positive big, respectively. Similarly, the fuzzy subset of the output variables is described as {VL, L, M, H, VH}, which specifically refers to the five levels of very low, low, medium, high, and very high, respectively. The parameters of the fuzzy control input and output are shown in Table 1. Taking the position control x direction as an example, the membership function of the designed position input and output is shown in Fig. 3.

Table 1 Parameter domain selection for the input and output of the FSMC

Variable	Input or output
$\boldsymbol{e}_x$	[−0.02, 0.02]
$\dot{\boldsymbol{e}}_x$	[−0.013, 0.013]
$\boldsymbol{e}_y$	[−0.02, 0.02]
$\dot{\boldsymbol{e}}_y$	[−0.013, 0.013]
$\boldsymbol{e}_z$	[−0.013, 0.013]
$\dot{\boldsymbol{e}}_z$	[−0.05, 0.05]
$\boldsymbol{\varepsilon}_{\boldsymbol{\chi}\mathrm{F}}$	[0.1, 3.9]
$\boldsymbol{k}_{\boldsymbol{\chi}\mathrm{F}}$	[20, 40]

Considering that when the UAV is subjected to a large interference, the system state will deviate significantly from the designed sliding mode surface, a situation that severely degrades control accuracy. Therefore, a controller with self-learning ability is designed based on fuzzy logic, and the formation of fuzzy logic rules is the core problem of the FSMC. To solve interference in the tracking process, the parameters can be self-adjusted based on the tracking error. For example, in the case of large interference, the adjustment parameters are increased to strengthen the control effect; on the contrary, in the case of small interference, the control parameters are reduced to achieve accurate tracking (Yang CY et al., 2018).

In addition, the analysis of the error $\boldsymbol{e}_{\boldsymbol{\chi}}$ and its rate of change $\dot{\boldsymbol{e}}_{\boldsymbol{\chi}}$ can be developed as the self-learning rule in the proposed FSMC. When $\boldsymbol{e}_{\boldsymbol{\chi}}\dot{\boldsymbol{e}}_{\boldsymbol{\chi}} > 0$, the error is rapidly moving away from the target $\boldsymbol{e}_{\boldsymbol{\chi}} = \mathbf{0}$. To tackle this problem, the values of parameters $\boldsymbol{\varepsilon}_{\boldsymbol{\chi}\mathrm{F}}$ and $\boldsymbol{k}_{\boldsymbol{\chi}\mathrm{F}}$ in the FSMC should be increased. On the contrary, the parameters that require self-learning should be reduced when the situation is $\boldsymbol{e}_{\boldsymbol{\chi}}\dot{\boldsymbol{e}}_{\boldsymbol{\chi}} < 0$, which indicates that the error is approaching the target. It should be noted that

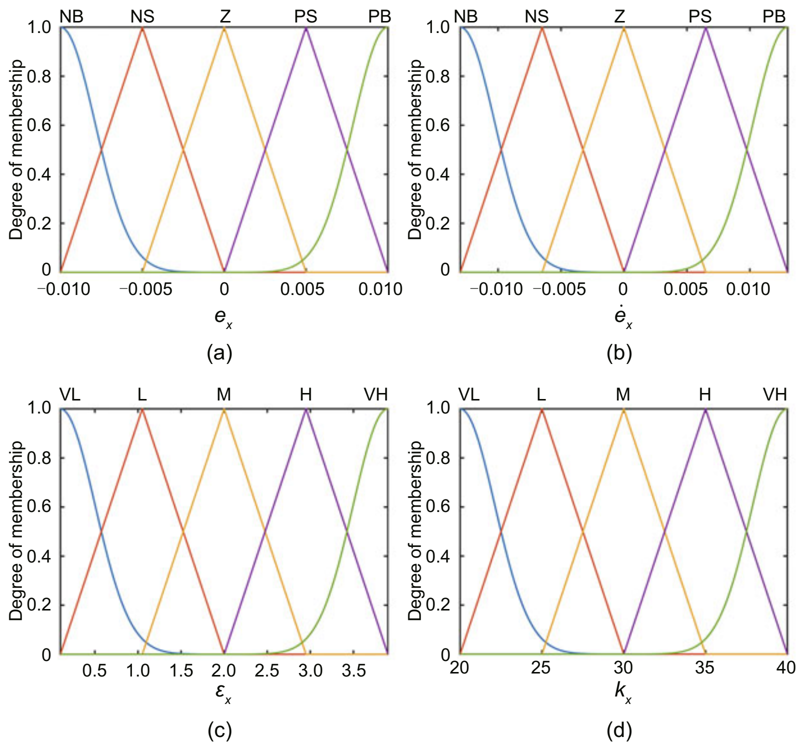

Fig. 3 Graph of the membership functions for the inputs and outputs: (a) $\boldsymbol{e_x}$; (b) $\dot{\boldsymbol{e}}_{\boldsymbol{x}}$; (c) $\boldsymbol{\varepsilon_x}$; (d) $\boldsymbol{k_x}$

.

when $\boldsymbol{e}_{\boldsymbol{\chi}} = \mathbf{0}$ and $\dot{\boldsymbol{e}}_{\boldsymbol{\chi}} = \mathbf{0}$, the error has reached its expected state, and the parameters do not need to be changed at this time. Then, based on the aforementioned analysis, through manual design based on model analysis, the fuzzy reasoning rules are shown in Table 2, and some fuzzy reasoning rules are extracted as

$$\begin{aligned} &\text{IF } \boldsymbol{e}_{\boldsymbol{\chi}} \text{ is PB and } \dot{\boldsymbol{e}}_{\boldsymbol{\chi}} \text{ is PB,}\\ &\text{THEN } \boldsymbol{\varepsilon}_{\boldsymbol{\chi}_{\mathrm{F}}} \text{ is VH and } \boldsymbol{k}_{\boldsymbol{\chi}_{\mathrm{F}}} \text{ is VH;}\\ &\text{IF } \boldsymbol{e}_{\boldsymbol{\chi}} \text{ is PB and } \dot{\boldsymbol{e}}_{\boldsymbol{\chi}} \text{ is NB,}\\ &\text{THEN } \boldsymbol{\varepsilon}_{\boldsymbol{\chi}_{\mathrm{F}}} \text{ is H and } \boldsymbol{k}_{\boldsymbol{\chi}_{\mathrm{F}}} \text{ is H;}\\ &\text{IF } \boldsymbol{e}_{\boldsymbol{\chi}} \text{ is Z and } \dot{\boldsymbol{e}}_{\boldsymbol{\chi}} \text{ is Z,}\\ &\text{THEN } \boldsymbol{\varepsilon}_{\boldsymbol{\chi}_{\mathrm{F}}} \text{ is M and } \boldsymbol{k}_{\boldsymbol{\chi}_{\mathrm{F}}} \text{ is M.} \end{aligned} \tag{13}$$

Table 2 Antecedent matrix for adaptive fuzzy adjustment of parameters $\boldsymbol{\varepsilon}_{\boldsymbol{\chi}_{\mathrm{F}}}$ and $\boldsymbol{k}_{\boldsymbol{\chi}_{\mathrm{F}}}$

$\boldsymbol{e}_{\boldsymbol{\chi}}$	$\dot{\boldsymbol{e}}_{\boldsymbol{\chi}}$				
	NB	NS	Z	PS	PB
NB	VH	VH	VL	H	H
NS	VH	VH	L	H	H
Z	VH	VH	M	VH	VH
PS	H	H	L	VH	VH
PB	H	H	VL	VH	VH

Then, based on the defined parameters, e.g., sliding mode surface (9), saturation function (11), and the self-learning parameters $\boldsymbol{\varepsilon}_{\boldsymbol{\chi}_{\mathrm{F}}}$ and $\boldsymbol{k}_{\boldsymbol{\chi}_{\mathrm{F}}}$, the intelligent control method using FSMC for the UAVs described by Eq. (5) can be described as

$$\boldsymbol{u}_{\mathrm{s}}(t) = \boldsymbol{A}^{-1}\left[-\boldsymbol{\varepsilon}_{\boldsymbol{\chi}_{\mathrm{F}}}\mathbf{sat}(\boldsymbol{s}_{\boldsymbol{\chi}}) - \boldsymbol{k}_{\boldsymbol{\chi}_{\mathrm{F}}}\boldsymbol{s}_{\boldsymbol{\chi}} + \boldsymbol{F} + \hat{\boldsymbol{d}}_{\mathrm{ext}}\right], \tag{14}$$

where $\boldsymbol{F} = \ddot{\boldsymbol{\chi}}_{\mathrm{d}} - \boldsymbol{c}_{\boldsymbol{\chi}}\dot{\boldsymbol{e}}_{\boldsymbol{\chi}} - \boldsymbol{f}_1(\cdot)$ and $\hat{\boldsymbol{d}}_{\mathrm{ext}} = \bar{\boldsymbol{d}}_{\mathrm{ext}} - \boldsymbol{d}_{\mathrm{ext}}(\boldsymbol{\chi}, t)$.

3.2 Stability analysis

In this subsection, the study of the system stability based on external uncertainty is proved, which is crucial for the process of parameter self-learning.

Theorem 1 Under the assumption that the proposed control strategy described by Eq. (14) is adopted for the underactuated dynamic UAVs, the Lyapunov candidate function

$$\boldsymbol{V} = \frac{1}{2}\boldsymbol{s}_{\boldsymbol{\chi}}^2 \tag{15}$$

is adopted to validate the stability under Assumptions 1 and 2. If the parameters are adjusted in the designed FSMC self-learning control algorithm, i.e., $\boldsymbol{\varepsilon}_{\boldsymbol{\chi}_{\mathrm{F}}}$ and $\boldsymbol{k}_{\boldsymbol{\chi}_{\mathrm{F}}}$ satisfying

$$\boldsymbol{\varepsilon}_{\boldsymbol{\chi}_{\mathrm{F}}} \leq \boldsymbol{s}_{\boldsymbol{\chi}}\boldsymbol{k}_{\boldsymbol{\chi}_{\mathrm{F}}} - \bar{\boldsymbol{d}}_{\mathrm{ext}}, \tag{16}$$

then the tracking error $\boldsymbol{e}_{\boldsymbol{\chi}}$ is ensured to be ultimately uniformly bounded (UUB) in a complex flight environment.

Proof Please refer to the supplementary materials. The Lyapunov-based analysis establishes that regardless of the selected sliding mode surface type, the system state converges to a bounded region within a finite time. This guarantees that the tracking error remains within a fixed boundary for all subsequent time, satisfying the UUB stability criterion.

4 Simulations

To verify the control effect of the proposed FSMC strategy, simulations are conducted on the position of the quadrotor with interference using MATLAB/Simulink. The corresponding UAV parameters involved in the simulations are shown in Table 3 (Song et al., 2019).

Table 3 Corresponding parameters of the UAV used in the simulations

Variable	Value	Unit
m	2.00	kg
l	0.20	m
b	1.14	10^{-7} N·s^2/rad^2
κ	2.98	10^{-6} N·s^2/rad^2
ξ_x, ξ_y, ξ_z	1.20	10^{-2} N·s^2/rad^2
ξ_ϕ, ξ_θ, ξ_ψ	1.20	10^{-2} N·s^2/rad^2
I_x	1.25	N·s^2/rad^2
I_y	1.25	N·s^2/rad^2
I_z	2.50	N·s^2/rad^2

The UAV position reference trajectory is designed as

$$\boldsymbol{\chi}_{\mathrm{d}}(t) = \left[5\left(1-\cos\left(\frac{\pi}{10}t\right)\right), 5\sin\left(\frac{\pi}{10}t\right), 5\left(1-\mathrm{e}^{-0.3t}\right)\right]^{\mathrm{T}},$$

where $\boldsymbol{\chi}_{\mathrm{d}} = [x_{\mathrm{d}}(t), y_{\mathrm{d}}(t), z_{\mathrm{d}}(t)]^{\mathrm{T}}$ and the yaw angle reference track is set to $\boldsymbol{\psi}_{\mathrm{d}} = \mathbf{0}$. Based on the set trajectory, the terminal time of the simulations is set to 60 s, and the step size is 0.001. In the following content, control strategies, i.e., SMC, adaptive RBFNNC, and the proposed FSMC, are designed, and the corresponding comparative simulation results of the tracking accuracy and analysis are also demonstrated.

4.1 Tracking effect of SMC

Based on the selected Lyapunov function (15) and the designed parameters shown in Eqs. (9)–(11), the controller using SMC is designed:

$$\boldsymbol{u}_{\mathrm{s}}(t)=\frac{-\boldsymbol{\varepsilon}_{\boldsymbol{\chi}}\mathbf{sat}(\boldsymbol{s}_{\boldsymbol{\chi}})-\boldsymbol{k}_{\boldsymbol{\chi}}\boldsymbol{s}_{\boldsymbol{\chi}}+\boldsymbol{F}+\hat{\boldsymbol{d}}_{\mathrm{ext}}}{\boldsymbol{A}} \tag{17}$$

as a comparative control algorithm for FSMC, where $\boldsymbol{F}=\ddot{\chi}_{\mathrm{d}}-\boldsymbol{c}_{\boldsymbol{\chi}}\dot{\boldsymbol{e}}_{\boldsymbol{\chi}}-\boldsymbol{f}_1(\cdot)$. After multiple rounds of simulation debugging, the parameters $\boldsymbol{\varepsilon}_{\boldsymbol{\chi}}=[2,2,2]^{\mathrm{T}}$, $\boldsymbol{k}_{\boldsymbol{\chi}}=[30,30,30]^{\mathrm{T}}$, $\boldsymbol{c}_{\boldsymbol{\chi}}=[20,20,20]^{\mathrm{T}}$, and $\boldsymbol{\varDelta}_{\boldsymbol{\chi}}=[1,1,1]^{\mathrm{T}}$ are selected.

4.2 Tracking effect of adaptive RBFNNC

An adaptive RBFNNC algorithm, which combines the adaptive fault-tolerant NNC method with the RBFNNC algorithm, is also adopted to contrast simulations with the proposed FSMC for the UAVs. Taking $\boldsymbol{x}_i=\left[\chi_{\mathrm{d}i},\chi_i\right]$ as the input of RBF, where $\boldsymbol{x}_i$ is the i^{th} input vector and the output $f(\boldsymbol{x}_i)$ of the RBF acts on the sum of uncertainties $\boldsymbol{L}_1(\cdot)$ in the adaptive fault-tolerant NNC, then the control law can be described as (Song et al., 2019)

$$\boldsymbol{u}_{\mathrm{s}}=-\left(k_1+\frac{1}{2}\right)\boldsymbol{s}_1-c_1\hat{\alpha}_1\boldsymbol{s}_1\theta_1^2, \tag{18}$$

where k_1 and c_1 are the positive constant gains, $\hat{\alpha}_1$ is the estimate of a virtual parameter, $\boldsymbol{s}_1$ is a filtered variable, and θ_1 is the Gaussian basis function of the RBF neural network.

Corresponding tracking simulations are implemented under the setting of $n=50$ neurons, Gaussian parameters $\mu=0$ and $\iota=3$, and controller gains $k_1=2$ and $k_2=50$.

4.3 Tracking effect of the FSMC

4.3.1 Evaluation of the self-learning parameters

Specifically, the reason for the effectiveness of the proposed FSMC method in tracking accuracy compared with traditional SMC algorithms can be understood as that the system parameters $\boldsymbol{\varepsilon}_{\boldsymbol{\chi}_{\mathrm{F}}}$ and $\boldsymbol{k}_{\boldsymbol{\chi}_{\mathrm{F}}}$ have intelligent characteristics of self-learning control under complex working environments. The corresponding adjustment of the relevant parameters in the control process is shown in Fig. 4. To sum up, in the process of parameters' self-learning of the fuzzy module of the proposed FSMC, the curves of parameters $\boldsymbol{\varepsilon}_{x_{\mathrm{F}}}$ and $\boldsymbol{\varepsilon}_{y_{\mathrm{F}}}$ exhibit an overall stable trend due to the small external disturbances of the UAVs. However, due to the presence of nonlinear elements, these parameters experience brief fluctuations during specific time periods.

For example, the $\boldsymbol{\varepsilon}_{x_{\mathrm{F}}}$ curve exhibits an approximate 3-s fluctuation, with an amplitude of approximately 0.2, during the time periods of 10–20 s, 30–40 s, and 50–60 s. The $\boldsymbol{\varepsilon}_{y_{\mathrm{F}}}$ curve also exhibits similar fluctuations during the time periods of 0–10 s, 20–30 s, and 40–50 s. The amplitude of $\boldsymbol{\varepsilon}_{z_{\mathrm{F}}}$ curve is around 3.6, accompanied by a significantly small fluctuation with an amplitude of about 0.4 throughout the entire process, indicating that the nonlinear component has a more significant impact on $\boldsymbol{\varepsilon}_{z_{\mathrm{F}}}$ parameters. Similarly, Fig. 4b shows that the $\boldsymbol{k}_{x_{\mathrm{F}}}$ and $\boldsymbol{k}_{y_{\mathrm{F}}}$ curves exhibit similar trends to the $\boldsymbol{\varepsilon}_{x_{\mathrm{F}}}$ and $\boldsymbol{\varepsilon}_{y_{\mathrm{F}}}$ curves in Fig. 4a, but with an increase in the fluctuation amplitude. During the corresponding time period, the short-term fluctuation amplitudes of $\boldsymbol{k}_{x_{\mathrm{F}}}$ and $\boldsymbol{k}_{y_{\mathrm{F}}}$ curves are about 1.2. At the same time, the $\boldsymbol{k}_{z_{\mathrm{F}}}$ curve is the most significantly affected by nonlinearity, with amplitude fluctuations ranging from approximately 35 to 38 throughout the entire process, which are significant and frequent.

According to the above conclusions combined with the designed FSMC designed by Eq. (14), the parameter $\boldsymbol{k}$ related to the sliding mode surface needs to be adjusted in a large range within the nonlinear local range to achieve high-precision tracking effect. In contrast, the saturation function of the sliding mode surface $\boldsymbol{\varepsilon}$ only needs to be adjusted in a small range to realize this target due to the most demanding situations, i.e., step-driven signal on the z axis.

4.3.2 Evaluation of the accuracy of FSMC

In the simulations using the FSMC strategy, the parameters are set as $\boldsymbol{c}_{\boldsymbol{\chi}}=\mathbf{20}$ and $\boldsymbol{\varDelta}_{\boldsymbol{\chi}}=\mathbf{1}$. Additionally, two other parameters, $\boldsymbol{\varepsilon}_{\boldsymbol{\chi}_{\mathrm{F}}}$ and $\boldsymbol{k}_{\boldsymbol{\chi}_{\mathrm{F}}}$, are dynamically tuned by the designed FLM, and their value ranges are detailed in Table 1.

To validate the superiority of the proposed FSMC in achieving high tracking accuracy and enhanced disturbance rejection in the UAV positioning system, comparative simulations are conducted against the adaptive RBFNNC strategies and conventional SMC. It should be noted that in actual flight, external disturbances cannot be ignored. To further validate the robustness of the proposed method, random disturbances are introduced into the simulation environment. The simulation results of the UAV position tracking curves and their tracking errors are shown in Fig. 5, with Fig. 5b derived based on Eq. (8). The tracking curves in Fig. 5a show that the designed FSMC is closest to the reference curves in the three positional trajectories compared with other control methods, confirming its superior trajectory tracking accuracy. In Fig. 5b, due to the function approximation characteristics of the neu-

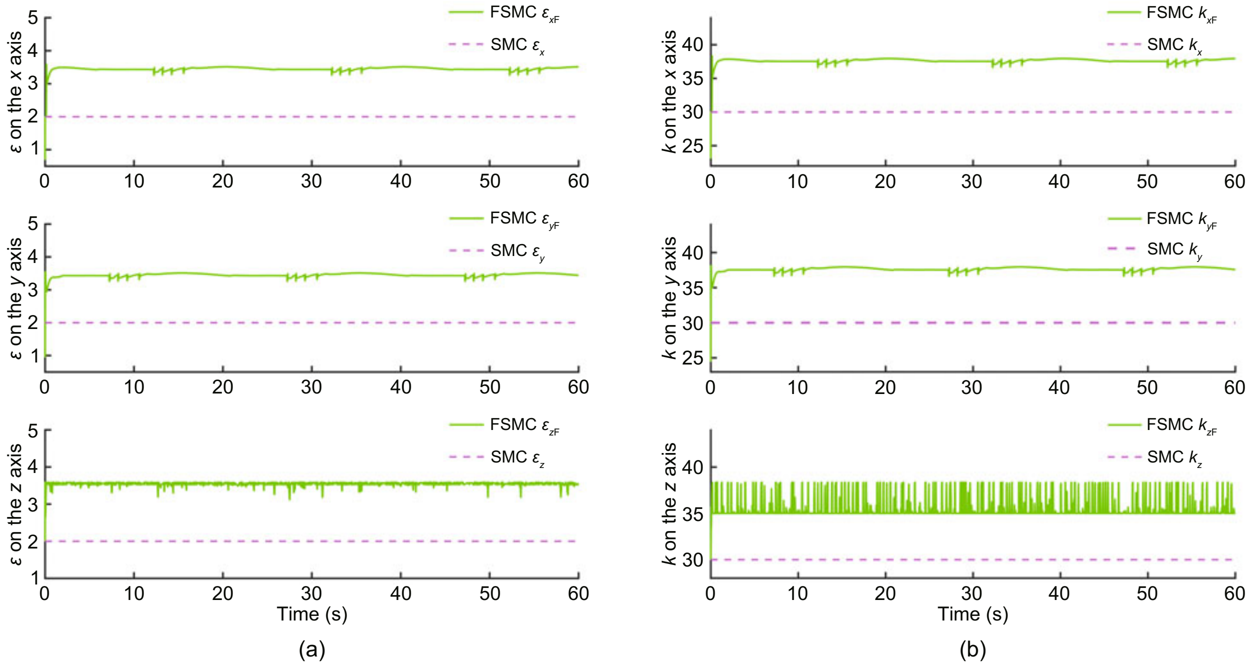

Fig. 4 Parameter values in the UAV position system: (a) FSMC strategy parameter $\boldsymbol{\varepsilon}_{\chi\mathrm{F}}$ and SMC parameter $\boldsymbol{\varepsilon}_{\chi}$; (b) FSMC strategy parameter $\boldsymbol{k}_{\chi\mathrm{F}}$ and SMC parameter $\boldsymbol{k}_{\chi}$ ($\boldsymbol{\varepsilon}_{\chi\mathrm{F}} = [\varepsilon_{x_\mathrm{F}}, \varepsilon_{y_\mathrm{F}}, \varepsilon_{z_\mathrm{F}}]^\mathrm{T}$ and $\boldsymbol{k}_{\chi\mathrm{F}} = [k_{x_\mathrm{F}}, k_{y_\mathrm{F}}, k_{z_\mathrm{F}}]^\mathrm{T}$)

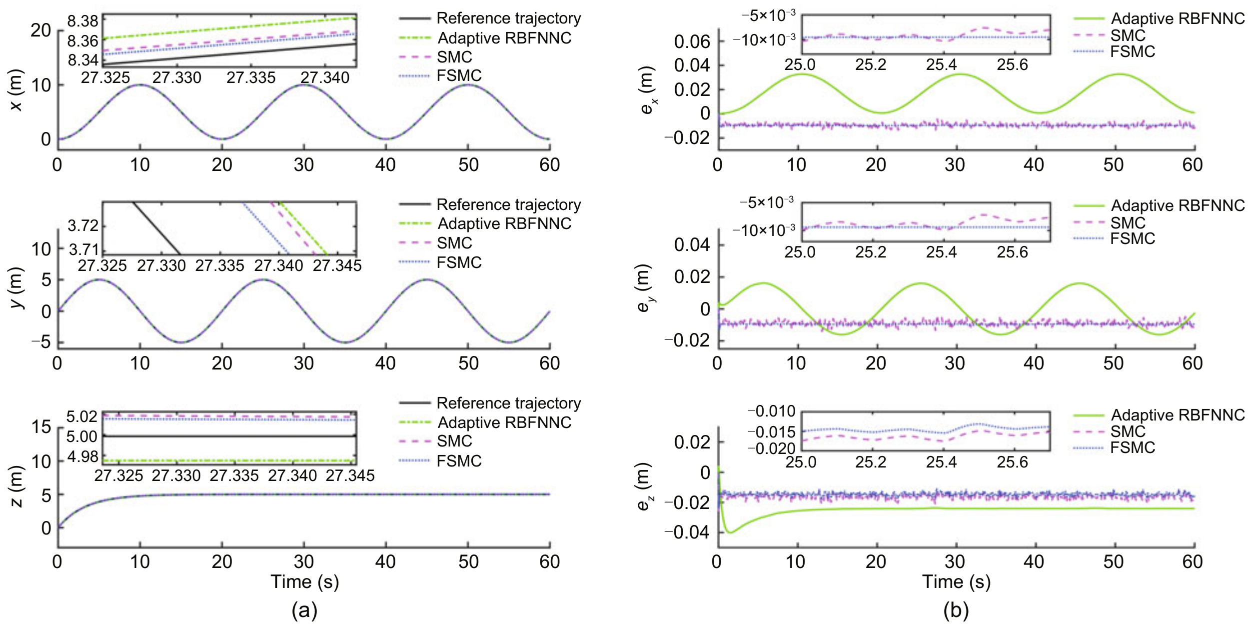

Fig. 5 Position tracking performance for UAVs: (a) the effect of position tracking; (b) the error of position tracking

ral network, the error curve of RBFNNC exhibits fluctuation patterns similar to the rate of change in the reference trajectory. The traditional SMC and FSMC exhibit zero-baseline band oscillation errors due to the boundary layer effect of SMC. However, FSMC effectively suppresses oscillation amplitudes across all position control directions through the fuzzy adaptive mechanism, achieving a maximum reduction of 67.97% (see quantitative analysis below for details).

To accurately capture the maximum deviation between the actual and reference trajectories in Fig. 5, the maximum absolute error (MaxAE) is used as the primary key metric. In contrast, error fluctuation (EF) is used to reflect the range of error variation across controllers. The results are shown in Table 4. The MaxAE values for FSMC in the x, y, and z directions are 10.497, 13.666, and 24.092 mm, respectively, which are all lower than those of SMC (14.369, 14.222, and 26.312 mm) and RBFNNC (32.768, 16.223, and 40.147 mm). Similarly, the EF values for FSMC in the x, y, and z directions are 10.497, 14.162, and 24.092 mm, respectively, smaller than those of the other controllers. This demonstrates that FSMC not only minimizes trajectory errors but also effectively suppresses EFs, thereby significantly improving the tracking accuracy and system stability.

Given the complexity of the UAV motion in a three-dimensional (3D) space, Fig. 6 provides a 3D trajectory tracking plot, offering a more intuitive depiction of the UAV's flight path. To further quantify differences throughout the control process, error evaluation metrics such as mean square error (MSE) and mean absolute error (MAE) are introduced, as summarized in Table 5. These metrics capture the cumulative impact of small deviations over the control cycle, providing a more comprehensive analysis of the system accuracy and stability (Bodmann and Singh, 2011).

Fig. 6 illustrates that the actual trajectory under the FSMC strategy closely aligns with the reference trajectory, and its MSE and MAE are the lowest among all strategies, as shown in Table 5, demonstrating its trajectory tracking robustness in multi-degree-of-freedom coordinated control. Specifically, FSMC achieves an MSE of 4.04×10^{-4} m^2 and an MAE of 3.4105×10^{-2} m, which are significantly lower than those of the other control methods. This reflects the high efficiency and accuracy of FSMC in minimizing error. Compared to SMC, FSMC reduces MSE by 9.21% and MAE by 1.90%. When compared to the adaptive RBFNNC, FSMC achieves a substantial reduction of 65.88% in MSE and 34.55% in MAE. These precisely quantified results indicate FSMC's superior performance in enhancing tracking accuracy, system stability, and robustness, providing a more reliable and efficient control scheme for practical applications.

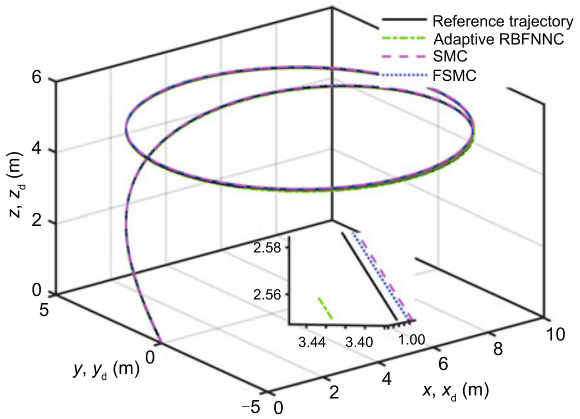

Fig. 6 State position tracking trajectory in a 3D space

Table 5 MSE and MAE values for trajectory tracking under different control strategies

Control strategy	MSE ($\times10^{-4}$ m^2)	MAE ($\times10^{-2}$ m)
Adaptive RBFNNC	11.84	5.2106
SMC	4.45	3.4764
FSMC	4.04	3.4105

Table 4 MaxAE and EF values for trajectory tracking in the x, y, and z directions under different control strategies

Control strategy	x direction		y direction		z direction	
	MaxAE (mm)	EF (mm)	MaxAE (mm)	EF (mm)	MaxAE (mm)	EF (mm)
Adaptive RBFNNC	32.768	32.768	16.223	32.283	40.147	44.091
SMC	14.369	14.369	14.222	14.716	26.312	26.312
FSMC	10.497	10.497	13.666	14.162	24.092	24.092

5 Conclusions

A novel intelligent FSMC strategy with self-learning and self-adapting abilities for UAV positioning and tracking is addressed. To improve the robustness and stability of the system in the presence of external disturbances and model uncertainties, fuzzy logic is adopted to tune the parameters of the traditional SMC. Moreover, using filter variables and their rates of change as the input of the fuzzy submodel of FSMC, adaptive tuning of SMC parameters to environmental changes is achieved through FLM+SMC, which also effectively mitigates the chattering phenomenon commonly observed in conventional SMC during control processes. The stability of the FSMC system is validated using the Lyapunov theory, and simulation results confirm significant improvements in the trajectory tracking accuracy and error robustness when compared to conventional SMC and adaptive RBFNNC strategies. The technical features of the FSMC demonstrate its significant potential for UAV systems where high precision and reliability are critical.

Despite demonstrating notable advantages and potential, the proposed FSMC strategy still has certain limitations. Its effectiveness has been validated solely through numerical simulations, without simulation verification on a physical UAV platform. As a result, its practical feasibility and robustness under real-world uncertainties and hardware constraints remain unproven. A promising direction for future research is the integration of fault-tolerant control mechanisms, which could enhance the system resilience to actuator and sensor failures, thereby improving the overall reliability and applicability of the strategy to real-world applications.

Contributors

Ruiwen XIANG designed the research. Qingmei CAO and Ruiwen XIANG drafted the paper. Qingmei CAO supervised the project, provided guidance, and revised the paper. Yonghong TAN, Weiqing SUN, and Xiaodong ZHOU reviewed the paper and provided substantial suggestions. Jiawei CHI assisted in the methodology design. Lei YAO helped organize and revise the paper. Ruiwen XIANG finalized the paper.

Conflict of interest

All the authors declare that they have no conflict of interest.

Data availability

The data that support the findings of this study are available within the paper and the electronic supplementary materials.

References

Amer A, Mehndiratta M, le Fevre Sejersen J, et al., 2023. Visual tracking nonlinear model predictive control method for autonomous wind turbine inspection. 21st Int Conf on Advanced Robotics, p.431-438. https://doi.org/10.1109/ICAR58858.2023.10406329

Bodmann BG, Singh PK, 2011. Burst erasures and the mean-square error for cyclic Parseval frames. *IEEE Trans Inform Theory*, 57(7):4622-4635. https://doi.org/10.1109/TIT.2011.2146150

Chen FY, Jiang RQ, Zhang KK, et al., 2016. Robust backstepping sliding-mode control and observer-based fault estimation for a quadrotor UAV. *IEEE Trans Ind Electron*, 63(8):5044-5056. https://doi.org/10.1109/TIE.2016.2552151

Chen PY, Zhang GB, Guan T, et al., 2021. The motion controller based on neural network S-plane model for fixed-wing UAVs. *IEEE Access*, 9:93927-93936. https://doi.org/10.1109/ACCESS.2021.3093768

Du HB, Zhu WW, Wen GH, et al., 2019. Distributed formation control of multiple quadrotor aircraft based on nonsmooth consensus algorithms. *IEEE Trans Cybern*, 49(1):342-353. https://doi.org/10.1109/TCYB.2017.2777463

Ermeydan A, Kiyak E, 2017. Fault tolerant control against actuator faults based on enhanced PID controller for a quadrotor. *Aircr Eng Aerosp Technol*, 89(3):468-476. https://doi.org/10.1108/AEAT-04-2015-0096

Guo XT, Hou SJ, Niu PJ, et al., 2022. A review of control methods for quadrotor UAVs. 5th Int Conf on Electronics and Electrical Engineering Technology, p.132-138. https://doi.org/10.1109/EEET58130.2022.00030

Jiang M, 2021. Application of fuzzy PID control in UAV control system. 3rd Int Conf on Inventive Research in Computing Applications, p.197-200. https://doi.org/10.1109/ICIRCA51532.2021.9544986

Li YJ, Huynh DV, Nguyen VL, et al., 2024. Multiagent UAV-aided URLLC mobile edge computing systems: a joint communication and computation optimization approach. *IEEE Syst J*, 18(4):1828-1838. https://doi.org/10.1109/JSYST.2024.3426096

Mendoza AMER, Yu W, 2023. Fuzzy adaptive control law for trajectory tracking based on a fuzzy adaptive neural PID controller of a multi-rotor unmanned aerial vehicle. *Int J Contr Autom Syst*, 21(2):658-670. https://doi.org/10.1007/s12555-021-0299-2

Nair AP, Selvaganesan N, Lalithambika VR, 2016. Lyapunov based PD/PID in model reference adaptive control for satellite launch vehicle systems. *Aerosp Sci Technol*, 51:70-77. https://doi.org/10.1016/j.ast.2016.01.017

Nguyen NP, Mung NX, Thanh HLNN, et al., 2021. Adaptive sliding mode control for attitude and altitude system of a quadcopter UAV via neural network. *IEEE Access*, 9:40076-40085. https://doi.org/10.1109/ACCESS.2021.3064883

Nodland D, Zargarzadeh H, Jagannathan S, 2013. Neural network-based optimal adaptive output feedback control of a helicopter UAV. *IEEE Trans Neur Netw Learn Syst*, 24(7):1061-1073. https://doi.org/10.1109/TNNLS.2013.2251747

Pounds PEI, Bersak DR, Dollar AM, 2012. Stability of small-scale UAV helicopters and quadrotors with added payload mass under PID control. *Auton Robots*, 33(1-2):129-142. https://doi.org/10.1007/s10514-012-9280-5

Rahbari D, Ahmed F, Jenihhin M, et al., 2024. Reliability-critical computation offloading in UAV swarms. *IEEE Syst J*, 18(4):1871-1882. https://doi.org/10.1109/JSYST.2024.3432449

Rao JJ, Li B, Zhang Z, et al., 2022. Position control of quadrotor UAV based on cascade fuzzy neural network. *Energies*, 15(5):1763. https://doi.org/10.3390/en15051763

Santoso F, Garratt MA, Anavatti SG, 2021. Hybrid PD-fuzzy and PD controllers for trajectory tracking of a quadrotor unmanned aerial vehicle: autopilot designs and real-time flight tests. *IEEE Trans Syst Man Cybern Syst*, 51(3):1817-1829. https://doi.org/10.1109/TSMC.2019.2906320

Shen SY, Xu JF, 2021. Adaptive neural network-based active disturbance rejection flight control of an unmanned helicopter. *Aerosp Sci Technol*, 119:107062-107073. https://doi.org/10.1016/j.ast.2021.107062

Song YD, He L, Zhang D, et al., 2019. Neuroadaptive fault-tolerant control of quadrotor UAVs: a more affordable solution. *IEEE Trans Neur Netw Learn Syst*, 30(7):1975-1983. https://doi.org/10.1109/TNNLS.2018.2876130

Wang F, He S, Zhou C, et al., 2024. Distributed practical finite-time formation control of quadrotor UAVs based on finite-time event-triggered disturbance observer. *IEEE Syst J*, 18(1):355-366. https://doi.org/10.1109/JSYST.2023.3331300

Wang T, Xie WF, Zhang YM, 2014. Sliding mode reconfigurable control using information on the control effectiveness of actuators. *J Aerosp Eng*, 27(3):587-596. https://doi.org/10.1061/(ASCE)AS.1943-5525.0000240

Yang CY, Shen LP, Zhou LN, 2018. Fuzzy sliding mode control for permanent magnet synchronous motors. 5^{th} Int Conf on Information, Cybernetics, and Computational Social Systems, p.331-336. https://doi.org/10.1109/ICCSS.2018.8572331

Yang L, Wu LG, Lv YY, et al., 2023. Combined MPC and dynamic neural network-based UAVs trajectory tracking control. *IEEE Access*, 11:145763-145771. https://doi.org/10.1109/ACCESS.2023.3343770

Yu L, He G, Wang XK, et al., 2022. Robust fixed-time sliding mode attitude control of tilt trirotor UAV in helicopter mode. *IEEE Trans Ind Electron*, 69(10):10322-10332. https://doi.org/10.1109/TIE.2021.3118556

List of supplementary materials

1 Proof of Theorem 1